Measurements of branching fraction and direct CP asymmetry in $B^{\pm} \to K_s^0 K_s^0 K^{\pm}$ and a search for $B^{\pm} \to K_s^0 K_s^0 \pi^{\pm}$ at Belle

Abdul Basith K

Indian Institute of Technology, Madras

7 May 2019
TIFR, Mumbai

Outline of the talk

- Introduction
- Motivation
- Experimental setup
- Signal reconstruction
- Background studies
- Signal extraction
- Results and summary

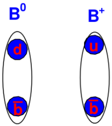

Why B mesons.?

$\rightarrow$ An ideal environment for the measurements of CKM matrix elements, CP violation parameters and to look for possible new physics effects

CP violation and CKM Matrix:

Charge conjugation (C) and parity (P) operation $\rightarrow$ symmetry between particles and antiparticles

$$V_{\rm CKM} = \begin{pmatrix} V_{ud} & V_{us} & V_{ub} \\ V_{cd} & V_{cs} & V_{cb} \\ V_{td} & V_{ts} & V_{tb} \end{pmatrix} \cong \begin{pmatrix} 1-\lambda^2/2 & \lambda & A\lambda^3(\rho - i\eta) \\ -\lambda & 1-\lambda^2/2 & A\lambda^2 \\ A\lambda^3(1-\rho-i\eta) & -A\lambda^2 & 1 \end{pmatrix}$$

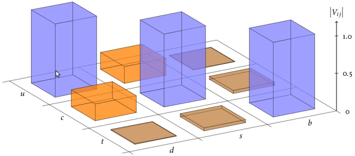

Magnitudes of CKM matrix elements.

- A 3 x 3 complex unitary matrix
- $|V_{ij}|$ represents the strength of the quark level transition
- The complex phase accounts for CP violation in the standard model (SM)

Types of *CP* violation

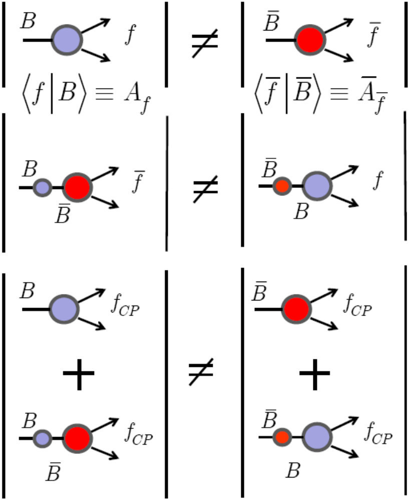

$$\left|\frac{\bar{A}_{\bar{f}}}{A_f}\right| \neq 1$$

direct CP violation

(charged and neutral B mesons)

$$\left|\frac{q}{p}\right| \neq 1$$

CP violation via mixing

(only neutral B mesons)

CP violation via interference between mixing and decay (“mixing-induced CPV”)

$$\mathrm{Im}\,\frac{q}{p}\frac{\bar{A}_f}{A_f} \neq 0$$

(only neutral B mesons)

Motivation

- Charmless decays of B mesons to three body final states:

$$B^+ \longrightarrow K_s^0 K_s^0 K^+ \; (b \rightarrow s \text{ transition})$$
$$B^+ \longrightarrow K_s^0 K_s^0 \pi^+ \; (b \rightarrow d \text{ transition})$$

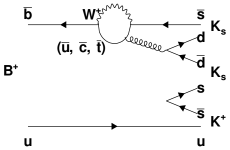

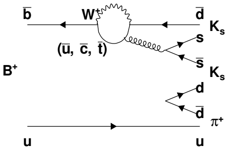

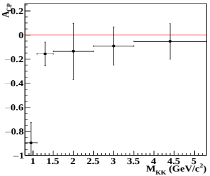

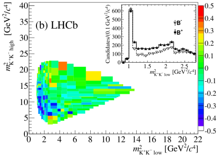

→ Sensitive to possible non-SM contributions

→ Opportunity to study two-body intermediate resonances and to search for any localized CP asymmetry

→ Recent results on $B^{\pm} \rightarrow K^+K^-K^{\pm}$, $K^+K^-\pi^{\pm}$ etc. report strong evidence for large CP asymmetry at low K^+K^- invariant mass regions[1].

[1](Belle Collaboration) Phys. Rev. D **96**, 031101(R), (LHCb Collaboration) Phys. Rev. Lett. **112**, 011801

Current status

Table: $B^{\pm} \to K_S^0 K_S^0 K^{\pm}$

Exp.	Data	Signal yield	B.F.($\times 10^{-6}$)	$\mathcal{A}_{CP}$
Belle[1]	78 fb^{-1}	66.5 ± 9.3	$13.4 \pm 1.9 \pm 1.5$	-
BaBar[2]	426 fb^{-1}	636 ± 28	$10.6 \pm 0.5 \pm 0.3$	$(4^{+4}_{-5} \pm 2)$ %

Table: $B^{\pm} \to K_S^0 K_S^0 \pi^{\pm}$

Exp.	Data	Signal yield	B.F.
Belle[1]	78 fb^{-1}	-1.8 ± 7.7	$< 3.2 \times 10^{-6}$
BaBar[3]	423.7 fb^{-1}	15 ± 15	$< 5.1 \times 10^{-7}$

- With full Belle dataset and updated systematic measurements we can have more precise measurements.

---

1 Phys. Rev. D **69**, 012001 (2004).

2 Phys. Rev. D **85**, 112010 (2012).

3 Phys. Rev. D **79**, 051101 (R) (2009).

KEKB and dataset

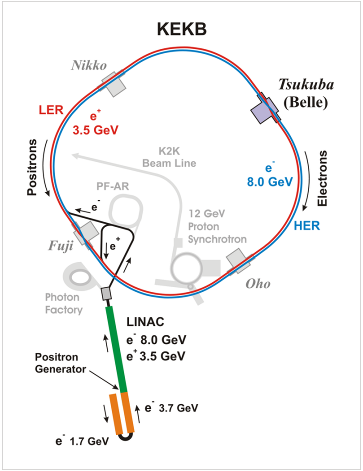

- KEKB is an asymmetric e^+e^- collider at the High Energy Accelerator Research Organization (KEK), Japan.
- 8.0 GeV e^- collides to 3.5 GeV e^+ at the $\Upsilon(4S)$ resonance
- Collected about 772 million $B\bar{B}$ till 2010
- The main goal was to search for CP violation in B meson decays

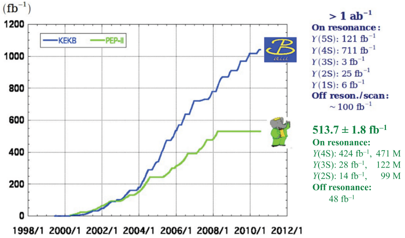

[1] Picture: https://belle.kek.jp/

Belle detector[1]

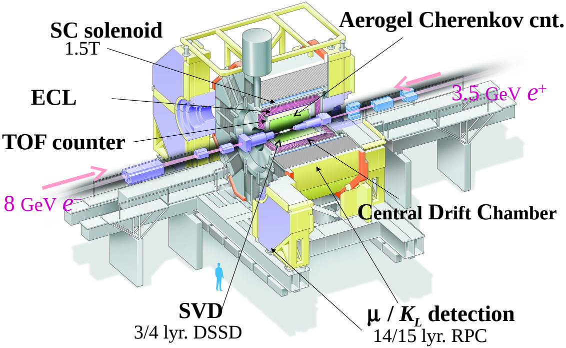

- The sub-detectors relevant for our study are: SVD, CDC, ACC and TOF

[1]Picture: https://belle.kek.jp/

Analysis strategy

- Follow a blind analysis technique: all the selection criteria need to be determined with Monte Carlo (MC) samples to avoid possible bias because of the analysts prior knowledge about the data

- Reconstruct $B^{\pm}$ candidates from $K_s^0 K_s^0 K^{\pm}$ and $K_s^0 K_s^0 \pi^{\pm}$
- Candidate selection using various kinematic variables
- Background studies using MC samples
- Use $B^+ \to \bar{D}^0(K_s^0 \pi^- \pi^+)\pi^+$ as a control mode
- 2D simultaneous extended maximum likelihood fit to determine the branching fraction ($\mathcal{B}$) and direct CP asymmetry ($\mathcal{A}_{CP}$)
- Obtain $\mathcal{B}$ and $\mathcal{A}_{CP}$ as a function of $M_{K_S^0 K_S^0}$ for $B^{\pm} \to K_s^0 K_s^0 K^{\pm}$

Signal MC studies

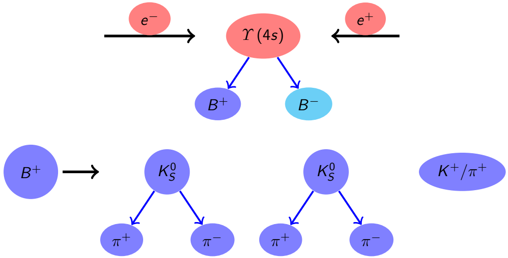

- A Monte Carlo simulated data sample is produced in two steps:

(1) Generate a complete decay chain using EvtGen program

(2) Simulate the detector response to these generated events with Geant3 based simulation package

Signal reconstruction

- B candidates are reconstructed by combining two K_S^0 candidates with one charged kaon or pion
- Use kinematic informations (ΔE and $M_{\rm bc}$) for the signal candidate selection
- Selection requirements:

Variable	Cut
$\|dr\|$	< 0.2 cm
$\|dz\|$	< 5.0 cm
$L(K/\pi)$	> 0.6 (Kaon) & < 0.4 (Pion)
K_S^0 mass	$\pm 3\sigma$ from the world average
ΔE	$-0.10 < \Delta E < 0.15\,\mathrm{GeV}$
$M_{\rm bc}$	$5.271 < M_{\rm bc} < 5.287\,\mathrm{GeV}/c^2$

dr & *dz*: Distance of closest approach with respect to the interaction point

$L(K/\pi)$: Kaon likelihood against the pion

ΔE: Energy difference

$M_{\rm bc}$: Beam constrained mass

$$M_{bc} = \sqrt{E^{*2}_{\rm BEAM} - \vec{p}^{\,*2}_{B}}$$

$$\Delta E = E^*_B - E^*_{\rm BEAM}$$

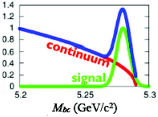

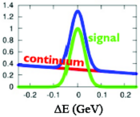

K_s^0 selection

- Reconstructed in the channel $K_s^0 \to \pi^+\pi^-$
- Use information from inner tracking system
- Reconstruct from pairs of oppositely charged tracks (assumed to be pions) that come from a common vertex
- Invariant mass of the track pairs to be within $\pm 3\sigma$ from the nominal K_s^0 mass

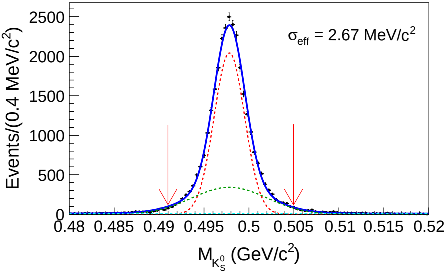

Mass distribution of K_s^0 candidates.

Background studies

Three types of backgrounds:

1. $e^+e^- \longrightarrow q\bar{q}$ ($q = u, d, s, c$) continuum processes
2. Charmed B decays ($b \to c$ transitions)
3. Charmless B decays ($b \to u, d, s$ transitions)

Continuum background

- The dominant background is from continuum processes

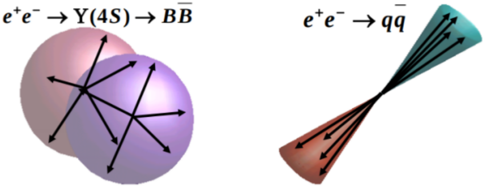

- Use the difference in event topology to suppress this background
- B mesons are almost at rest in the CM frame and thus decay without any preferred direction
- For continuum events, the quarks are moving fast away from each other resulting in jetlike events
- Combine event topology with other variables in a Neural Network

Continuum fighting variables

cosθ_{B}: cosine of the angle between the B momentum and the z axis

cosθ_{Bt}: cosine of the angle between the B thrust and the z axis

$\mathbf{R}_2$: Ratio of the 2nd and the 0th Fox-Wolfram moments

LR : Likelihood ratio using KSFW

cosθ_{thr}: cosine of the angle between the B and the non-B thrust axis

$\boldsymbol{\Delta} z$: Distance between the reconstructed and the tag B vertices along the z axis

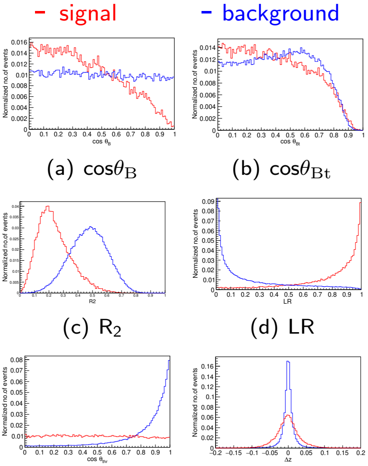

(a) cosθ_{B} (b) cosθ_{Bt}

(c) R_2 (d) LR

(e) cosθ_{thr} (f) Δz

For $B^+ \to K_S^0 K_S^0 K^+$ channel; similar for $B^+ \to K_S^0 K_S^0 \pi^+$.

NN output

- NN output ($C_{\rm NB}$) shows clear discrimination between signal and background
- $C_{\rm NB}$ is difficult to parametrize using some simple PDF
- Transformed as:

$$C'_{\rm NB} = \ln\left(\frac{C_{\rm NB} - C_{{\rm N}B,min}}{C_{{\rm N}B,max} - C_{\rm NB}}\right)$$

$$C_{{\rm N}B,min} = -0.2 \ \& \ C_{{\rm N}B,max} \sim 1.0$$

- 91% signal efficiency with 84% background rejection

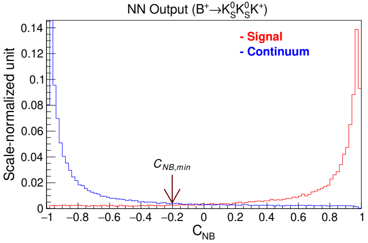

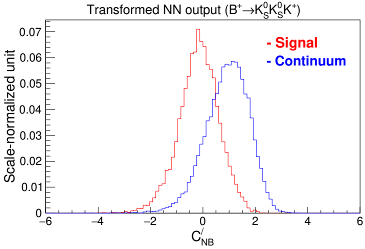

Charmed B background

- Found peaking structures in ΔE and $M_{\rm bc}$ signal regions

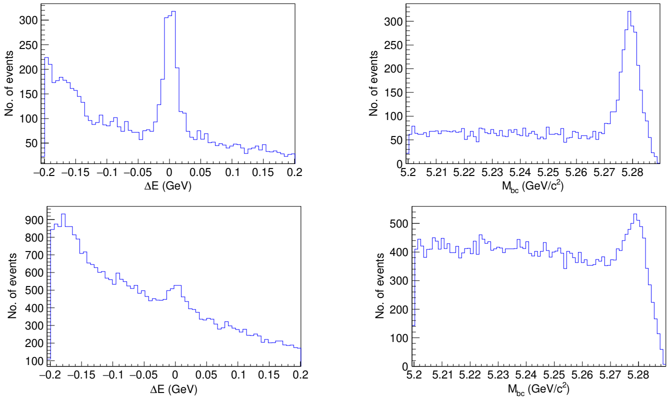

Figure: Distributions of ΔE and $M_{\rm bc}$ in Charmed B MC sample for $B^+ \to K_S^0 K_S^0 K^+$ (top) $B^+ \to K_S^0 K_S^0 \pi^+$ (bottom).

- Vetoes: $B^+ \to D^0 K^+$ and $B^+ \to \chi_{c0}(1P)K^+$

Veto windows:

$D^0 \to [1.85, 1.88]\,\mathrm{GeV}/c^2$

$\chi_{c0}(1P) \to [3.38, 3.45]\,\mathrm{GeV}/c^2$

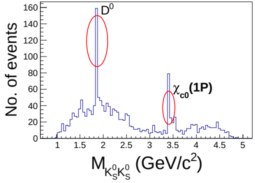

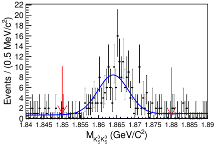

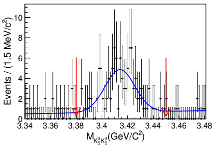

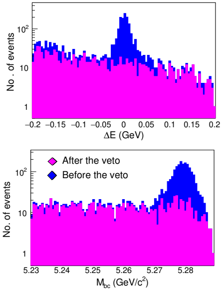

Figure: ΔE and M_{bc} before and after the veto

$\to$ Loss of signal efficiency due to the charm veto: $\simeq 3\%$

Charmed B background: $B^+ \to K_S^0 K_S^0 \pi^+$

- Veto: $B^+ \to D^0 \pi^+$

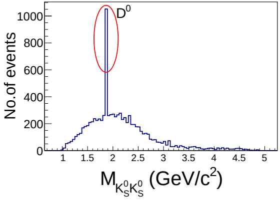

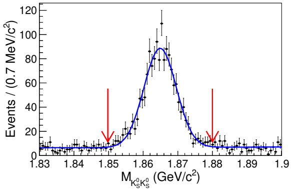

Veto window:

$D^0 \to [1.85, 1.88]\,\mathrm{GeV}/c^2$

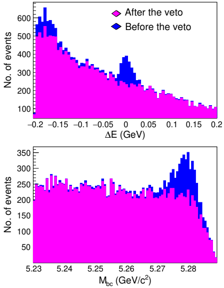

Figure: ΔE and $M_{\rm bc}$ before and after the veto

$\to$ Loss of signal efficiency due to the charm veto: $\simeq 1\%$

Charmless B background

$\rightarrow$ Combinatorial B: No peaking structure in the signal region

$\rightarrow$ Feed-across: Events with $K_S^0 K_S^0 \pi^+$ ($K_S^0 K_S^0 K^+$) final states for $B^+ \rightarrow K_S^0 K_S^0 K^+$ ($B^+ \rightarrow K_S^0 K_S^0 \pi^+$)

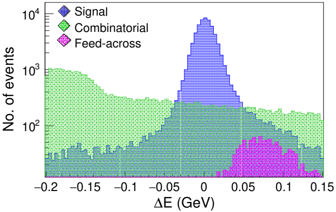

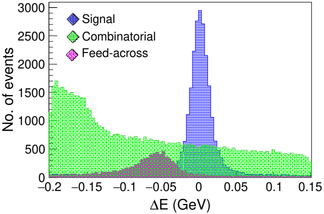

ΔE distribution in charmless B MC sample for $B^+ \rightarrow K_S^0 K_S^0 K^+$ (left) and $B^+ \rightarrow K_S^0 K_S^0 \pi^+$ (right).

- Total events: signal, continuum ($q\bar{q}$), feed-across and combinatorial B backgrounds.

Efficiency and expected yield

$$N_{exp}(B \to K_S^0 K_S^0 h) \approx \mathcal{B}(B \to K_S^0 K_S^0 h) \times \mathcal{B}(K_S^0 \to \pi^+\pi^-)^2 \times \varepsilon_{\rm rec} \times N_{B\bar{B}}$$

Table: Efficiency and expected yields for signal and feed-across modes.

Mode	$\varepsilon_{\rm rec}(\%)$	Yield
$B^+ \to K_S^0 K_S^0 K^+$	24.25 ± 0.02	954
$B^+ \to K_S^0 K_S^0 \pi^+$	27.51 ± 0.06	52
$B^+ \to K_S^0 K_S^0 \pi^+$ in $B^+ \to K_S^0 K_S^0 K^+$	1.49 ± 0.02	3
$B^+ \to K_S^0 K_S^0 K^+$ in $B^+ \to K_S^0 K_S^0 \pi^+$	2.39 ± 0.01	94

Table: Expected yields for the continuum and combinatorial B components obtained from MC.

Mode	Component	Yield
$B^+ \to K_S^0 K_S^0 K^+$	continuum	1722
	combinatorial B	120
$B^+ \to K_S^0 K_S^0 \pi^+$	continuum	3536
	combinatorial B	380

Fit preparation

- Define the branching fraction & inclusive CP asymmetry as:

$$\mathcal{B} = \frac{N_{\mathrm{sig}}}{\varepsilon_{\mathrm{rec}} \times N_{B\bar{B}} \times [\mathcal{B}(K_S^0 \to \pi^+\pi^-)]^2} \quad (1)$$

$$\mathcal{A}_{CP} = \frac{N_{B^-} - N_{B^+}}{N_{B^+} + N_{B^-}} \quad (2)$$

- Perform a 2D (ΔE-C'_{NB}) simultaneous fit to extract the signal yield for B^+ and B^-. The likelihood function $\mathcal{L}$ with probability density function, $\mathcal{P}_j^i$, is

$$\mathcal{L} = \frac{\mathrm{e}^{-\sum_j n_j}}{N!} \prod_i \Big[\sum_j n_j \mathcal{P}_j^i \Big], \quad \text{where} \quad \mathcal{P}_j^i \equiv \frac{1}{2}(1 - q^i \mathcal{A}_{CP,j}) \times \mathcal{P}_j(\Delta E^i) \times \mathcal{P}_j(C'^{\,i}_{\mathrm{NB}}) \quad (3)$$

Here i runs over events, n_j is the yield for the component j, q^i is the charge of the event and $\mathcal{P}_j$ is the PDF corresponds to the component j

- To account for crossfeed between the two channels, they are simultaneously fitted, with the $B^+ \to K_S^0 K_S^0 K^+$ branching fraction determining the normalization of the crossfeed in the $B^+ \to K_S^0 K_S^0 \pi^+$ fit region, and vice versa

2D fit: PDFs

Table: PDFs for $B^+ \to K_S^0 K_S^0 K^+$. G, AG and Poly1 denote a Gaussian, asymmetric Gaussian and a first-order polynomial

Event category	ΔE	C'_{NB}
Signal	3 G	G+AG
Continuum	Poly1	2G
Combinatorial B	Poly1	2G
Feed-across	G+Poly1	G

$\rightarrow$ An additional asymmetric Gaussian function for $B^+ \to K_s^0 K_s^0 \pi^+$ feed-across component

- **Free parameters in the fit:**
  - $\rightarrow$ branching fractions
  - $\rightarrow$ $\mathrm{N}_{\mathrm{q\bar{q}}}$
  - $\rightarrow$ $\mathcal{A}_{CP}(B^+ \to K_s^0 K_s^0 K^+)$
  - $\rightarrow$ PDF shape parameters for $q\bar{q}$ component
- $\mathcal{A}_{CP}$ for all other components are fixed to zero
- The combinatorial $B\overline{B}$ yields are fixed to their MC values
- The other PDF shape parameters for signal and background components are fixed from MC for both decays.

2D fit: projections

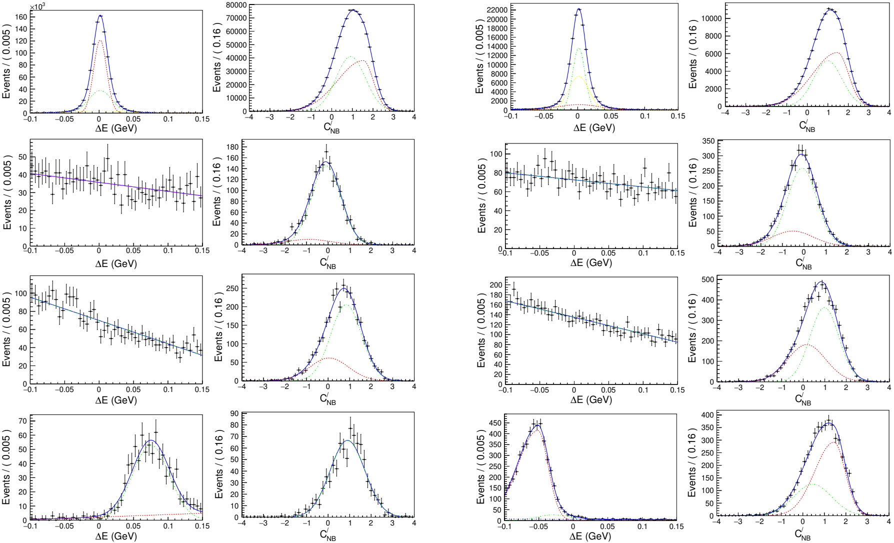

Fit validation

Pure toy test: PDF shapes are used to generate the toy data sets and these data then fitted with corresponding PDFs

GSIM test: Signal events are randomly extracted from the MC samples while all background events are generated from the PDF

$$\text{Pull} = \frac{\text{Fit yield} - \text{Expected yield}}{\text{Fit error}}$$

$\rightarrow$ If there is no bias in the fitter we expect the pull to be normally distributed with mean zero and width equal to one for all floated parameters

Linearity test: Ensemble tests are carried out with an assumed branching fraction/$\mathcal{A}_{CP}$ ranging from X to Y. Expect to get a straight line of unit slope and zero intercept if there is no bias

Fit validation: results

Table: Observed fit bias.

Mode	Pure toy (%)	GSIM (%)
$\mathcal{B}(B^+ \to K_S^0 K_S^0 K^+)$	-0.9	-0.8
$\mathcal{B}(B^+ \to K_S^0 K_S^0 \pi^+)$	-2.2	-4.0
$\mathcal{A}_{CP}(B^+ \to K_S^0 K_S^0 K^+)$	0.0	0.0

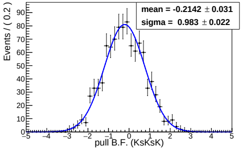

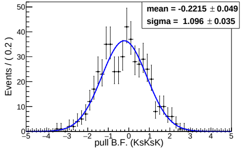

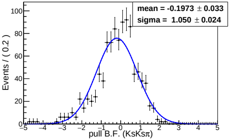

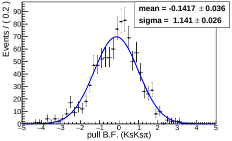

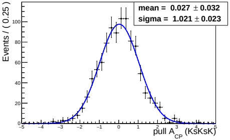

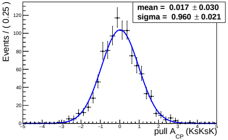

Fitted pull distributions from 1000 ensemble tests for the signal component.

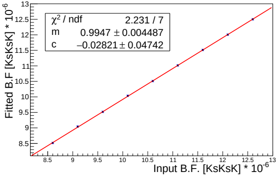

(a) $B^+ \to K^0_S K^0_S K^+$

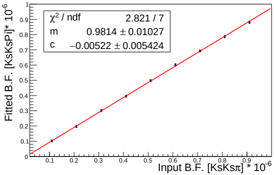

(b) $B^+ \to K^0_S K^0_S \pi^+$

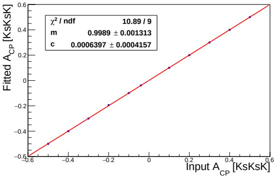

(c) $\mathcal{A}_{CP}(B^+ \to K^0_S K^0_S K^+)$

Control sample study

Goal: to determine possible data-MC difference in the fixed PDF shape parameters as well as to estimate the efficiency correction due to C_{NB} and M_{bc} requirements

- $B^+ \to \bar{D}^0\pi^+$ with $\bar{D}^0$ decays to $K_s^0\pi^+\pi^-$
- Similar final state as $B^+ \to K_s^0 K_s^0 \pi^+$ but has high statistics
- Perform a 2D (ΔE-C'_{NB}) fit to extract the signal yield of $B^+ \to \bar{D}^0\pi^+$

Fit results:

$\rightarrow$ Signal yield $= \mathbf{14,486 \pm 141}$

$$\mathcal{B}(B^+ \to \bar{D}^0\pi^+) = \frac{N_{\mathrm{yield}}}{\epsilon_{\mathrm{MC}} \times N_{B\bar{B}} \times \mathcal{B}(\bar{D}^0 \to K_S^0\pi\pi) \times \mathcal{B}(K_S^0 \to \pi\pi)}$$

$\rightarrow$ The obtained value of branching fraction for $B^+ \to \bar{D}^0\pi^+$ is $(\mathbf{4.50 \pm 0.32}) \times \mathbf{10^{-3}}$ which is consistent with the world average[1] value $(\mathbf{4.80 \pm 0.15}) \times \mathbf{10^{-3}}$.

1 Phys. Rev. D **98**, 030001 (2018).

Control sample study (Contd.)

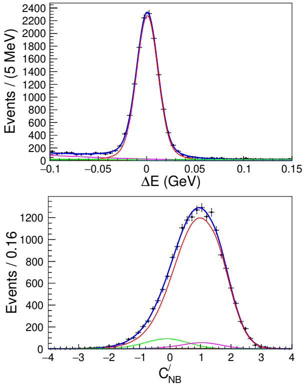

Figure: 2D fit projections for $B^+ \to \overline{D}^0\pi^+$ in total MC sample (left) and data (right)

Control sample study (Contd.)

Table: Correction factors for ΔE

Parameters	Data	MC	Correction factor
$\mu_1(GeV)$	0.0002 ± 0.0001	0.0007 ± 0.0001	-0.0005 ± 0.0002
$\sigma_1(GeV)$	0.0270 ± 0.0003	0.0228 ± 0.0002	1.1840 ± 0.0154

Table: Correction factors for C'_{NB}

Parameters	Data	MC	Correction factor
μ_2	0.8598 ± 0.0076	0.8542 ± 0.0069	0.0056 ± 0.0102
σ_2	0.7371 ± 0.0051	0.7275 ± 0.0047	1.0131 ± 0.0095

Efficiency correction due to requirements on NN output and M_{bc}:

- Compare the fit results with and without a cut

$$\varepsilon_{NB}^{\mathrm{data/MC}} = 0.997 \pm 0.014$$

$$\varepsilon_{M_{\mathrm{bc}}}^{\mathrm{data/MC}} = 1.0003 \pm 0.0475$$

Fit results in data: $B^{\pm} \to K_S^0 K_S^0 \pi^{\pm}$

- Data sample consists of 772×10^6 $B\overline{B}$ events
- Fit 5103 candidate events
- $\mathrm{N_{sig}} = 64 \pm 26$; $\mathrm{N_{q\bar{q}}} = 4574 \pm 75$

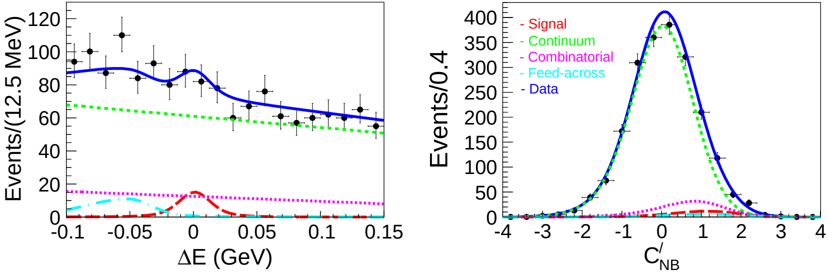

Figure: 2D simultaneous fit projections for $B^{\pm} \to K_S^0 K_S^0 \pi^{\pm}$ in data

Fit results in data: $B^{\pm} \to K_s^0 K_s^0 \pi^{\pm}$

$$\boxed{\mathcal{B}(B^+ \to K_s^0 K_s^0 \pi^+) = (6.5 \pm 2.6 \pm 0.4) \times 10^{-7}} \tag{4}$$

- Signal significance:

$$S = \sqrt{-2\ln(\mathcal{L}_0/\mathcal{L}_{\max})} \tag{5}$$

$\mathcal{L}_0$: Likelihood value for the fit with the signal yield fixed to zero

$\mathcal{L}_{\max}$: Likelihood for the best-fit case

- By convolving the likelihood with a Gaussian function of width equal to the systematic uncertainty: $S = 2.5\ \sigma$

- In the absence of a significant signal yield, we set a 90% confidence-level upper limit on the $\mathcal{B}$ at $\boxed{8.7 \times 10^{-7}}$ by integrating the convolved likelihood over the $\mathcal{B}$.

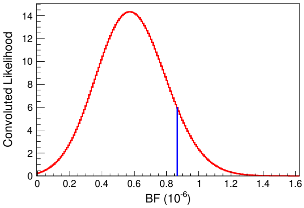

Convolved likelihood vs branching fraction.

Fit results in data: $B^{\pm} \to K_s^0 K_s^0 K^{\pm}$

- → Fit 2709 candidate events
- → $\mathrm{N_{sig}} = 902 \pm 44$
- → $\mathrm{N_{q\bar{q}}} = 1716 \pm 49$

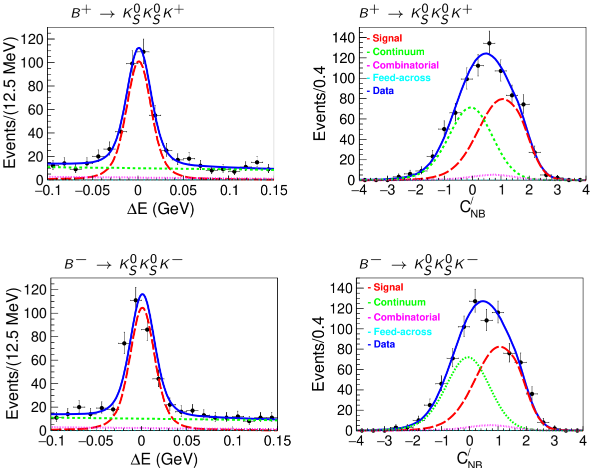

$\mathcal{B}$ and $\mathcal{A}_{CP}$ as a function of $M_{K_S^0 K_S^0}$ for $B^{\pm} \to K_S^0 K_S^0 K^{\pm}$

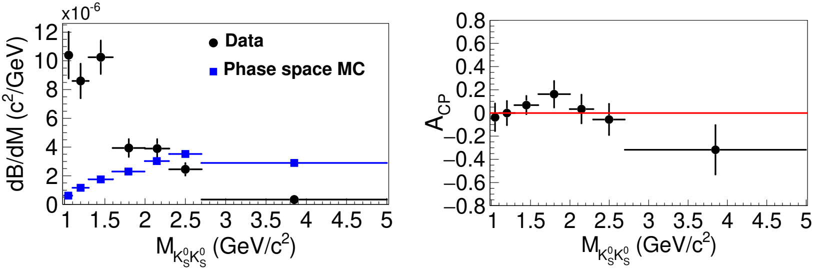

- Observed an excess of events at $M_{K_S^0 K_S^0} < 1.5\,\mathrm{GeV}/c^2$
- The results agree with BaBar that reported an $\mathcal{A}_{CP}$ consistent with zero as well as the presence of two-body intermediating resonances $f_0(980)$, $f_0(1500)$, and $f_2'(1525)$ in the low $M_{K_S^0 K_S^0}$ region[1]

[1] Phys. Rev. D **85**, 112010 (2012).

$\mathcal{B}$ and $\mathcal{A}_{CP}$ as a function of $M_{K_S^0 K_S^0}$ for $B^\pm \to K_S^0 K_S^0 K^\pm$

- Overall $\mathcal{B}$ and $\mathcal{A}_{CP}$:

$$\boxed{\mathcal{B}(K_s^0 K_s^0 K^\pm) = (10.42 \pm 0.43 \pm 0.22) \times 10^{-6}}$$

$$\boxed{\mathcal{A}_{CP} = (1.6 \pm 3.9 \pm 0.9)\%}$$

Table: Efficiency, differential branching fraction, and $\mathcal{A}_{CP}$ in $M_{K_S^0 K_S^0}$ bins.

$M_{K_S^0 K_S^0}$ (GeV/c^2)	Efficiency (%)	$d\mathcal{B}/dM \times 10^{-6}$ (c^2/GeV)	$\mathcal{A}_{CP}$ (%)
$1.0 - 1.1$	24.0 ± 0.4	$10.40 \pm 1.24 \pm 0.38$	$-3.9 \pm 10.9 \pm 0.9$
$1.1 - 1.3$	23.4 ± 0.2	$8.60 \pm 0.85 \pm 0.32$	$-0.1 \pm 9.3 \pm 0.9$
$1.3 - 1.6$	22.9 ± 0.1	$10.23 \pm 0.73 \pm 0.38$	$+6.6 \pm 6.9 \pm 0.9$
$1.6 - 2.0$	21.8 ± 0.1	$3.93 \pm 0.43 \pm 0.15$	$+16.1 \pm 10.3 \pm 0.9$
$2.0 - 2.3$	24.1 ± 0.1	$3.90 \pm 0.47 \pm 0.15$	$-3.3 \pm 11.3 \pm 0.9$
$2.3 - 2.7$	25.2 ± 0.1	$2.45 \pm 0.33 \pm 0.09$	$-5.7 \pm 12.2 \pm 1.0$
$2.7 - 5.0$	26.3 ± 0.0	$0.35 \pm 0.07 \pm 0.01$	$-31.9 \pm 19.7 \pm 1.2$

Systematic uncertainties

Table: Systematic uncertainties in the branching fraction of $B^+ \to K_S^0 K_S^0 \pi^+$.

Source	Relative uncertainty in $\mathcal{B}$ (%)
Tracking	0.35
Particle identification	0.80
Number of $B\overline{B}$ pairs	1.37
Continuum suppression	0.34
Requirement on $M_{\rm bc}$	0.03
K_S^0 reconstruction efficiency	3.22
Fit bias	1.86
Signal PDF	1.30
Combinatorial $B\overline{B}$ PDF	$+1.31, -1.98$
Feed-across PDF	$+3.57, -4.10$
Fixed background yield	$+2.63, -2.27$
Fixed background $\mathcal{A}_{CP}$	0.50
Total	$+6.30, -6.67$

Systematic uncertainties for $B^+ \to K_S^0 K_S^0 K^+$

$M_{K_S^0 K_S^0}$ (GeV/c^2)	1.0 − 1.1	1.1 − 1.3	1.3 − 1.6	1.6 − 2.0	2.0 − 2.3	2.3 − 2.7	2.7 − 5.0
Source	Relative uncertainty in $d\mathcal{B}/dM$ (%)						
Tracking†	0.35						
Particle identification†	0.80						
Number of $B\overline{B}$ pairs†	1.37						
Continuum suppression†	0.34						
Requirement on $M_{\rm bc}^\dagger$	0.03						
K_S^0 reconstruction†	3.22						
Fit bias†	0.53						
Signal PDF	$^{+0.33}_{-0.27}$	$^{+0.63}_{-0.48}$	$^{+0.46}_{-0.44}$	$^{+0.22}_{-0.63}$	$^{+0.52}_{-0.38}$	0.67	1.10
Combinatorial $B\overline{B}$ PDF	0.09	$^{+0.08}_{-0.13}$	0.12	$^{+0.17}_{-0.21}$	$^{+0.26}_{-0.34}$	0.40	0.40
Feed-across PDF	···	···	···	···	···	···	···
Fixed background yield	···	0.10	0.10	0.23	···	0.11	0.60
Fixed background $\mathcal{A}_{CP}$	···	···	···	0.20	0.10	···	0.13
Total	±3.68	±3.72	±3.69	±3.73	±3.72	±3.75	±3.89

$M_{K_S^0 K_S^0}$ (GeV/c^2)	1.0 − 1.1	1.1 − 1.3	1.3 − 1.6	1.6 − 2.0	2.0 − 2.3	2.3 − 2.7	2.7 − 5.0
Source	Absolute uncertainty in $\mathcal{A}_{CP}$						
Signal PDF	0.001	0.002	0.001	0.002	0.001	0.001	0.004
Combinatorial $B\overline{B}$ PDF	0.001	0.001	0.001	···	0.001	0.002	0.001
Feed-across PDF	···	···	···	···	···	···	···
Fixed background yield	···	···	0.001	0.001	0.001	0.001	0.004
Fixed background $\mathcal{A}_{CP}$	···	···	0.001	0.001	0.001	0.002	0.006
Detector bias†	0.009						
Total	±0.009	±0.009	±0.009	±0.009	±0.009	±0.010	±0.012

Results and summary

- In the absence of a significant signal yield, we obtain a 90% confidence-level upper limit on the branching fraction of $B^{\pm} \to K_S^0 K_S^0 \pi^{\pm}$ as: $\boxed{8.7 \times 10^{-7}}$

- Overall $\mathcal{B}.\mathcal{F}.$ and $\mathcal{A}_{CP}$ for $B^{\pm} \to K_S^0 K_S^0 K^{\pm}$ is obtained as:

$$\boxed{\mathcal{B}(K_S^0 K_S^0 K^{\pm}) = (10.42 \pm 0.43 \pm 0.22) \times 10^{-6}}$$

$$\boxed{\mathcal{A}_{CP} = (1.6 \pm 3.9 \pm 0.9)\%}$$

Phys. Rev. D **99**, 031102(R) (2019)

- Similar to BaBar, observed an excess of events at $M_{K_S^0 K_S^0} < 1.5\,\mathrm{GeV}/c^2$ of $B^{\pm} \to K_S^0 K_S^0 K^{\pm}$

- These supersede Belle's earlier measurements and constitute the most precise results to date
- Results are statistically dominated, hence a great prospect for Belle II

Belle II @ SuperKEKB

- A major upgrade of KEKB; designed to achieve 40 times higher peak luminosity
- Target luminosity: $8 \times 10^{35}\mathrm{cm}^{-2}\mathrm{s}^{-1}$
- Integrated luminosity $50\ \mathrm{ab}^{-1}$ (2019 to 2027)

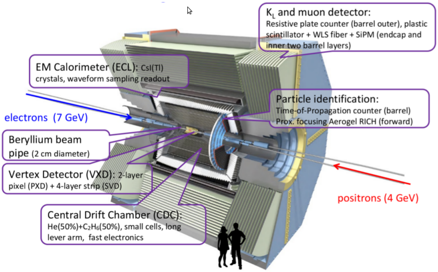

[2]

- All the sub-detectors of Belle are upgraded to cope up with the large amount of data and higher beam background
- Vertex detector (VXD): PXD + SVD is one of the key upgrade

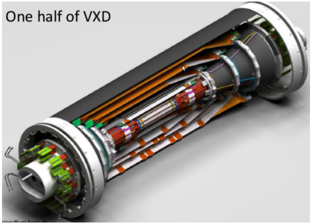

[2] T. Abe *et al.* (Belle II Collaboration), arXiv : 1011.0352 [physics.ins − det].

Software - Hardware mapping for Belle II SVD

- To prepare an xml file representing the connections between DSSD strips, APVs, and FADCs for SVD

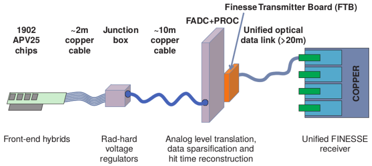

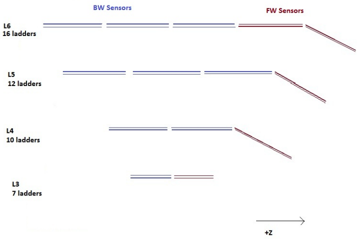

DSSDs	Type	No.of strips (p side)	No.of strips (n side)	No. of APVs per sensors (p side)	No. of APVs per sensors (n side)
Large	HPK	768	512	6	4
Trapezoidal	Micron	768	512	6	4
Small	HPK	768	768	6	6

FADCs...

	Ladders	BW sensors (per ladder)	FW sensors (per ladder)	BW sensors (total)	FW sensors (total)	BW FADCs	FW FADCs
L3	7	1 (HPK)	1 (HPK)	7 (HPK)	7(HPK)	1	1
L4	10	2 (HPK)	1 (Micron)	20(HPK)	10(Micron)	3	2
L5	12	3 (HPK)	1 (Micron)	36(HPK)	12(Micron)	5	2
L6	16	3 (HPK)	2 (HPK,Micron)	48(HPK)	16(HPK) + 16 (Micron)	6	4
total				111	61	15	9

• 24 FADCs for each p- and n-side, **total 48 FADCs**.

1

DSSD, APV and FADC numbering

- DSSD Strips : 000 to 767
- APV address from 0 to 47 (48 input channels for 1 FADC)
- 8 bit FADC address:

MSD						LSD
1 → n 0 0 → p	1 → BW 0 → FW	0 0 1 1	0 1 0 1	X	Y	Z

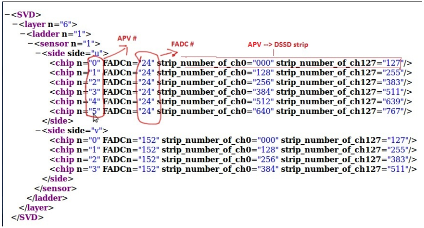


```
-<SVD>
 -<layer n="6">
  -<ladder n="1">
   -<sensor n="1">
    -<side side="u">
      <chip n="0" FADCn="24" strip_number_of_ch0="000" strip_number_of_ch127="127"/>
      <chip n="1" FADCn="24" strip_number_of_ch0="128" strip_number_of_ch127="255"/>
      <chip n="2" FADCn="24" strip_number_of_ch0="256" strip_number_of_ch127="383"/>
      <chip n="3" FADCn="24" strip_number_of_ch0="384" strip_number_of_ch127="511"/>
      <chip n="4" FADCn="24" strip_number_of_ch0="512" strip_number_of_ch127="639"/>
      <chip n="5" FADCn="24" strip_number_of_ch0="640" strip_number_of_ch127="767"/>
    </side>
    -<side side="v">
      <chip n="0" FADCn="152" strip_number_of_ch0="000" strip_number_of_ch127="127"/>
      <chip n="1" FADCn="152" strip_number_of_ch0="128" strip_number_of_ch127="255"/>
      <chip n="2" FADCn="152" strip_number_of_ch0="256" strip_number_of_ch127="383"/>
      <chip n="3" FADCn="152" strip_number_of_ch0="384" strip_number_of_ch127="511"/>
    </side>
   </sensor>
  </ladder>
 </layer>
</SVD>
```


Connection rules between FADCs and hybrids/ Origamis

- 24 FADCs for each p- and n-side, total 48 FADCs
- FADC $\longrightarrow$ 1 Junction board $\longrightarrow$ 8 hybrids/Origamis (at most)
- 1 hybrid/Origami reads out one side of a DSSD
- 1 FADC serves either p or n sides, but never both
- 1 FADC serves either FW or BW, but never both
- 1 FADC serves only hybrids in one layer
- 1 FADC serves either HPK or Micron, but never both
- 1 FADC $\longrightarrow$ 8 hybrids and 1 hybrid can have maximum 6 APVs

References

- A. Bevan *et al.*, Eur. Phys. J. C **74**, 3026 (2014).
- N. Cabibbo, Phys. Rev. Lett. **10**, 531 (1963); M. Kobayashi and T. Maskawa, Prog. Theor. Phys. **49**, 652 (1973).
- A. Abashian *et al.* (Belle Collaboration), Nucl. Instrum. Methods Phys. Res., Sect. A **479**, 117 (2002).
- S. Kurokawa and E. Kikutani, Nucl. Instrum. Methods Phys. Res., Sect. A **499**, 1 (2003).
- R. Aaij *et al.* (LHCb Collaboration), Phys. Rev. D **90**, 112004 (2014).
- R. Aaij *et al.* (LHCb Collaboration), Phys. Rev. Lett. **112**, 011801 (2014).
- C.-L. Hsu *et al.* (Belle Collaboration), Phys. Rev. D **96**, 031101(R) (2017).
- A. Garmash *et al.* (Belle Collaboration), Phys. Rev. D **69**, 012001 (2004).
- J. P. Lees *et al.* (BaBar Collaboration), Phys. Rev. D **85**, 112010 (2012).
- B. Aubert *et al.* (BaBar Collaboration), Phys. Rev. D **79**, 051101(R) (2009).

Thank You!

Back up: Best candidate selection

- More than one B candidate are reconstructed in some of the events
- The average multiplicity per event is 1.13 for $B^+ \to K_s^0 K_s^0 K^+$ and 1.49 for $B^+ \to K_s^0 K_s^0 \pi^+$
- Perform the K_s^0 and B vertex fit and the candidate having the minimum B vertex fit χ^2 is chosen as the best candidate in the event
- This criterion selects the correct B-meson candidate in 75% ($B^+ \to K_s^0 K_s^0 K^+$) and 63% ($B^+ \to K_s^0 K_s^0 \pi^+$) of events having multiple candidates.

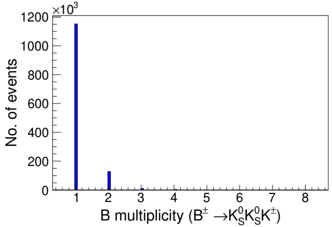

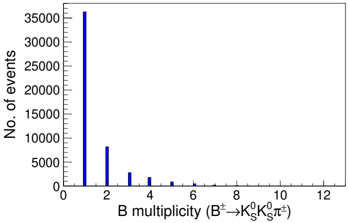

Back up : Fox Wolfram moments

The l^{th} order Fox-Wolfram moment H_l is defined as:

$$H_l = \sum_{i,j} \frac{|p_i||p_j|}{s} P_l(cos\ \theta_{ij}) \quad (6)$$

p_i & p_j : momenta of the i^{th} and j^{th} daughter particles in the event,
s : the square of the total energy of the event
P_l: Legendre polynomial of order l
$\theta_{i,j}$: the angle between the momenta of the particles.

Normalized Fox-Wolfram moment R_l:

$$R_l = \frac{H_l}{H_0} \quad (7)$$

These quantities describe the event topology of e^+e^- annihilations.

Back up: Neural Network (NN)[1]

- Difficult to take correlations into account in analysis based on multiple selections
- Multi variate analysis using NeuroBayes package
- Variables describing the event topology are combined in a NN

- **Analogy with brain:**

$\rightarrow$ Get input from other neurons
$\rightarrow$ Merge inputs
$\rightarrow$ Send the output

Three stage process:
Input layer $\rightarrow$ Hidden layer $\rightarrow$ Output layer

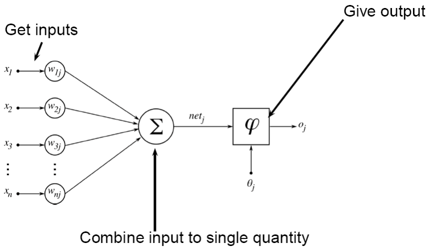

[1] Nucl. Instrum. Methods Phys. Res., Sect. A **559**, 190 (2006)

Bck up: Fit validation: $B^+ \to K_s^0 K_s^0 K^+$

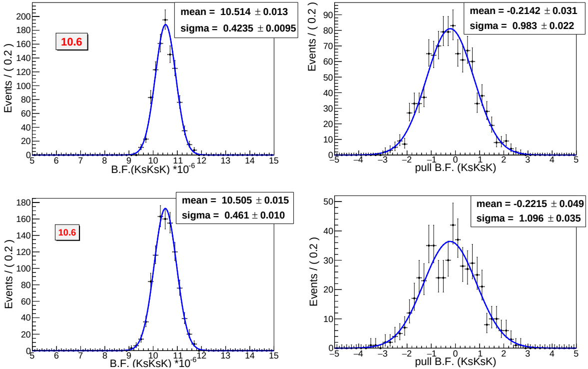

bias (GSIM): -0.9 %

bias (pure toy): -0.8 %

Fitted distribution of branching fraction (left) and corresponding pull (right) from 1000 GSIM (top) and pure toy (bottom) ensemble tests for the signal component of $B^+ \to K_S^0 K_S^0 K^+$.

Bck up: Fit validation: $B^+ \to K_s^0 K_s^0 \pi^+$

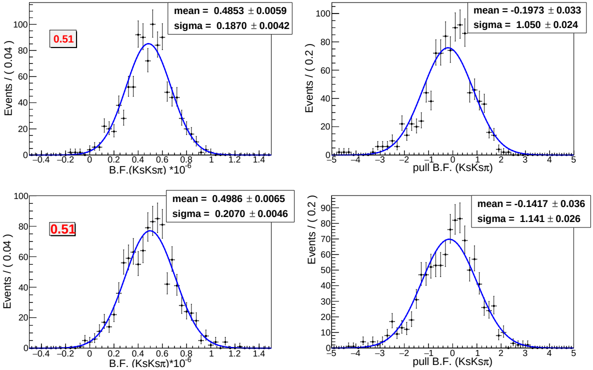

bias (GSIM): -4.0 %

bias (pure toy): -2.2 %

Fitted distribution of branching fraction (left) and corresponding pull (right) from 1000 GSIM (top) and pure toy (bottom) ensemble tests for the signal component of $B^+ \to K_S^0 K_S^0 \pi^+$.

Bck up: Fit validation for $\mathcal{A}_{CP}$

$\rightarrow$ $\mathcal{A}_{CP}$ is fixed to zero for all the components except $B^+ \rightarrow K^0_S K^0_S K^+$ signal

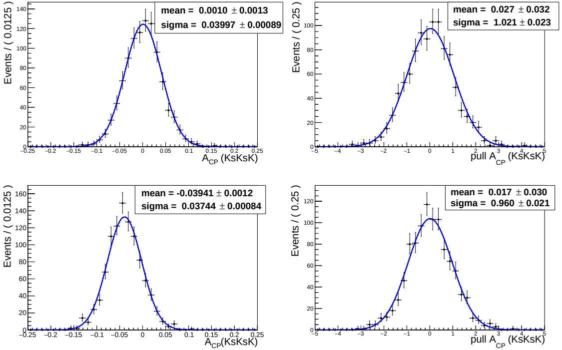

Fitted distributions of $\mathcal{A}_{CP}$ (left) and corresponding pull (right) from 1000 pure toy (top) and GSIM (bottom) ensemble tests for the $B^+ \rightarrow K^0_S K^0_S K^+$ sample.

Back up: Control sample study (Contd.)

Efficiency correction due to NN output requirement

- Compare the fit results with and without any cut on NN output.

- Take the ratio of number of events passes through both cases to calculate the efficiency correction ($\varepsilon_{NB}^{data/MC}$)

$$R = \frac{\text{signal yield in nominal case } (\text{NB}_{\text{min}}{=}-0.2)}{\text{signal yield with no cut on NB}}$$

$$R_{\text{data}} = 0.886 \pm 0.012 \tag{8}$$

$$R_{\text{MC}} = 0.889 \pm 0.003 \tag{9}$$

$$\varepsilon_{NB}^{\text{data/MC}} = 0.997 \pm 0.014 \tag{10}$$

$\rightarrow$ Efficiency correction due to M_{bc} requirement is calculated in a similar procedure:

$$\varepsilon_{M_{\text{bc}}}^{\text{data/MC}} = 1.0003 \pm 0.0475 \tag{11}$$

Back up:correlation

Table: Correlation coefficients for various fit components for $B^+ \to K_S^0 K_S^0 \pi^+$.

Components	ΔE - M_{bc}	M_{bc} - C'_{NB}	ΔE - C'_{NB}
Signal	-18.0 %	2.3 %	-2.1 %
Continuum	1.1 %	-1.7 %	0.3 %
Combinatorial B	-1.1 %	1.0 %	0.6 %
Feed-across	-46.9 %	8.7 %	-6.9 %

Back up : kaon-pion likelihood

Reconstructed based on the combined informations from the CDC, TOF, and ACC detectors

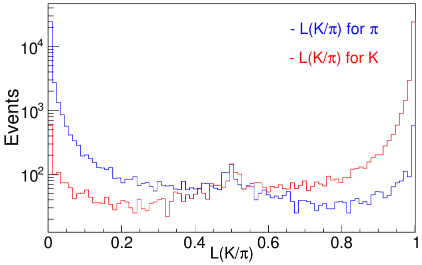

Figure: Distributions of kaon-pion likelihood

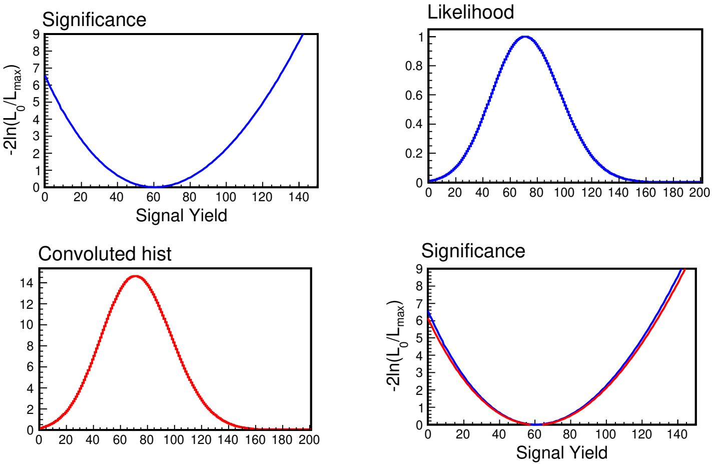

Figure: Projection plot of NLL and statistical likelihood for $B^+ \to K_S^0 K_S^0 \pi^+$. The blue curve shows statistical likelihood and the red curve shows convolved histogram.